Journal of Cellular Biochemistry 93:1033–1047 (2004)

Chromator, A Novel and Essential Chromodomain Protein Interacts Directly With the Putative Spindle Matrix Protein Skeletor

Uttama Rath, Dong Wang, Yun Ding, Ying-Zhi Xu, Hongying Qi, Melissa J. Blacketer, Jack Girton, Jørgen Johansen, and Kristen M. Johansen*

Department of Biochemistry, Biophysics, and Molecular Biology, Iowa State University, Ames, Iowa 50011

Abstract We have used a yeast two-hybrid interaction assay to identify Chromator, a novel chromodomain containing protein that interacts directly with the putative spindle matrix protein Skeletor. Immunocytochemistry demonstrated that Chromator and Skeletor show extensive co-localization throughout the cell cycle. During interphase Chromator is localized on chromosomes to interband chromatin regions in a pattern that overlaps that of Skeletor. However, during mitosis both Chromator and Skeletor detach from the chromosomes and align together in a spindle-like structure. Deletion construct analysis in S2 cells showed that the COOH-terminal half of Chromator without the chromodomain was sufficient for both nuclear as well as spindle localization. Analysis of P-element mutations in the *Chromator* locus shows that Chromator is an essential protein. Furthermore, RNAi depletion of Chromator in S2 cells leads to abnormal microtubule spindle morphology and to chromosome segregation defects. These findings suggest that Chromator is a nuclear protein that plays a role in proper spindle dynamics during mitosis. J. Cell. Biochem. 93: 1033–1047, 2004.

Key words: spindle matrix; mitosis; chromosomes; microtubules; *Drosophila*

A mitotic spindle is present in all known eukaryotic cells and its function is essential for proper chromosomal segregation and cell division to occur [reviewed in Mitchison and Salmon, 2001]. The spindle apparatus is a complex molecular machine known to be comprised of polymerized tubulin and various associated motor proteins [reviewed in Karsenti and Vernos, 2001]. Although much work has been directed towards understanding mitotic spindle apparatus structure and function, it is still unclear what directs and stabilizes the assembly of the spindle [Pickett-Heaps et al., 1997]. For these reasons and based on theoretical considerations of the requirement for force production at the spindle the concept of a spindle matrix has long been proposed [reviewed in Pickett-Heaps et al., 1982, 1997; Wells, 2001]. In its simplest formulation a spindle matrix is hypothesized to provide a more or less stationary substrate that provides a backbone or strut for motor molecules to interact with during force generation and microtubule sliding [Pickett-Heaps et al., 1997]. Such a matrix could also be envisioned to have the added properties of helping to organize and stabilize the microtubule spindle. However, direct molecular or biochemical evidence for such a matrix has been elusive [Scholey et al., 2001; Wells, 2001; Bloom, 2002; Johansen and Johansen, 2002; Kapoor and Compton, 2002].

In *Drosophila* we have recently identified a candidate spindle matrix protein that we named Skeletor [Walker et al., 2000]. Skeletor is an 81 kD protein that is associated with chromosomes at interphase but at prophase redistributes into a true fusiform spindle that precedes microtubule spindle formation [Walker et al., 2000]. During metaphase the "Skeletor-spindle" and the microtubule spindles are

Grant sponsor: National Science Foundation (to K.M.J.); Grant number: MCB0090877; Grant sponsor: Fung and Stadler graduate fellowship awards (to D.W., Y.-Z.X.).

*Correspondence to: Kristen M. Johansen, Department of Biochemistry, Biophysics, and Molecular Biology, 3154 Molecular Biology Building, Iowa State University, Ames, IA 50011. E-mail: kristen@iastate.edu

Received 19 May 2004; Accepted 18 June 2004

DOI 10.1002/jcb.20243

co-aligned. Importantly, during anaphase when the chromosomes segregate the Skeletor-defined spindle maintains its fusiform spindle structure from end to end across the midregion previously comprising the metaphase plate. At telophase the chromosomes start to decondense and reassociate with Skeletor where the two daughter nuclei are forming while Skeletor continues to also define a spindle in the midregion. When embryos are treated with nocodazole to disassemble the microtubules, the Skeletor spindle persists. Thus, the Skeletor-defined spindle exhibits many of the key properties predicted for the spindle matrix [Walker et al., 2000; Scholey et al., 2001; Wells, 2001; Johansen and Johansen, 2002]. However, Skeletor encodes a low-complexity protein with no obvious motifs making it unlikely that Skeletor itself is a structural component of a spindle matrix but rather that it is a member of a multi-protein complex. In searching for other members of such a complex we used a yeast two-hybrid screen to identify a protein directly interacting with Skeletor that we have named Chromator. Chromator contains a chromodomain and co-localizes with Skeletor on the chromosomes at interphase as well as to the Skeletor-defined spindle during metaphase. Furthermore, functional assays using P-element insertion mutants and RNAi in S2 cells suggest that Chromator is an essential protein that affects spindle function and chromosome segregation.

MATERIALS AND METHODS

Drosophila Stocks

Fly stocks were maintained according to standard protocols [Roberts, 1986]. Oregon-R or Canton-S was used for wild-type preparations. The $y^1; P\{y^{+mDint2} w^{BR.E.BR} = SUPor\text{-}P\}KG03258\ ry^{506}/TM3,\ Sb^1 Ser^1$ (*KG03258*) stock was obtained from the Bloomington *Drosophila* Stock Center and the $P\{y^{+mDint2}\ w^{BR.E.BR} = SUPor\text{-}P\}KG06256\ ry^{506}/TM3,\ Sb^1 Ser^1$ (*KG06256*) stock was obtained from the Baylor/BDGP Gene Disruption Project [Bellen et al., 2004]. The *y w; Δ2–3 Sb/TM2Ubx e* stock was the generous gift of Dr. Linda Ambrosio (Iowa State University).

Identification and Molecular Characterization of Chromator

Skeletor cDNA sequence (AF321290) containing residues 215–474 was subcloned in-frame into the yeast two hybrid bait vector pGBKT7 (Clontech, Palo Alto, CA) using standard methods [Sambrook et al., 1989] and verified by sequencing [Iowa State University (ISU) Sequencing Facility]. The Skeletor bait was used to screen the Clontech Matchmaker 0–21 h embryonic Canton-S yeast two-hybrid cDNA library according to the manufacturer's instructions as well as a *Drosophila* 0–2 h embryonic yeast two-hybrid library (the generous gift of Dr. L. Ambrosio, Iowa State University). Positive cDNA clones were isolated from both libraries, retransformed into yeast cells containing the Skeletor bait to verify the interaction, and sequenced. Homology searches identified the interacting clones as comprised of partial coding sequences from the *CG10712* locus. Several ESTs (RE33863, RE01873, RE35827, RE37221, LD39127, LD43522, GM27059, and SD06626) obtained from the Berkeley *Drosophila* Genome Project were sequenced and used to assemble the full-length Chromator coding sequence. The Chromator sequence was compared with known and predicted sequences using the National Center for Biotechnology Information BLAST e-mail server. The sequence was further analyzed using *SMART* (Simple Modular Architecture Research Tool; http://smart.embl-heidelberg.de/) to predict the domain organization of the protein.

Antibodies

Residues 601–926 and 1–260 of the predicted Chromator protein were subcloned using standard techniques [Sambrook et al., 1989] into the pGEX-4T-1 vector (Amersham Pharmacia Biotech, Piscataway, NJ) to generate the constructs GST-421 and GST-260. The correct orientation and reading frame of the inserts were verified by sequencing. The GST-421 and GST-260 fusion proteins were expressed in XL1-Blue cells (Stratagene, LaJolla, CA) and purified over a glutathione agarose column (Sigma-Aldrich, St. Louis, MO), according to the pGEX manufacturer's instructions (Amersham Pharmacia Biotech). The mAbs 6H11, 8D12, and 6A2 were generated by injection of 50 μg of GST-421 and the mAb 12H9 by injection of 50 μg of GST-260 into BALB/c mice at 21 d intervals. After the third boost, mouse spleen cells were fused with Sp2 myeloma cells and monospecific hybridoma lines were established using standard procedures [Harlow and Lane, 1988]. A mAb specific to GST, 8C7, was similarly generated. The mAb

6H11 is of the IgG1 subtype. All procedures for mAb production were performed by the Iowa State University Hybridoma Facility. The anti-Skeletor mAb 1A1 and Bashful antiserum have been previously described [Walker et al., 2000]. Anti-α-tubulin, anti-V5, and anti-GFP antibody were obtained from commercial sources (Sigma-Aldrich, Invitrogen, Carlsbad, CA and Molecular Probes, Eugene, OR, respectively).

Biochemical Analysis

SDS–PAGE and immunoblotting. SDS–PAGE was performed according to standard procedures [Laemmli, 1970]. Electroblot transfer was performed as in Towbin et al. [1979] with transfer buffer containing 20% methanol and in most cases including 0.04% SDS. For these experiments we used the Bio-Rad Mini PROTEAN II system, electroblotting to 0.2 μm nitrocellulose, and using anti-mouse HRP-conjugated secondary antibody (Bio-Rad, Hercules, CA) (1:3,000) for visualization of primary antibody diluted 1:1,000 in Blotto. The signal was visualized using chemiluminescent detection methods (ECL kit, Amersham Pharmacia Biotech). The immunoblots were digitized using a flatbed scanner (Epson Expression 1680). For quantification of immunolabeling, digital images of exposures of immunoblots on Biomax ML film (Kodak, Rochester, NY) were analyzed using the ImageJ software as previously described [Wang et al., 2001]. In these images the grayscale was adjusted such that only a few pixels in the wild type lanes were saturated. The area of each band was traced using the outline tool and the average pixel value determined. Levels in *KG06256* and *KG03258* mutant larvae were determined as a percentage relative to the level determined for wild type control larvae using tubulin levels as a loading control. In RNAi experiments Chromator levels were normalized using tubulin loading controls for each sample.

Pull-down experiments. For in vitro pull down assays, residues 215–474 of Skeletor was subcloned in-frame into the Pinpoint Xa-2 vector (Promega, Madison, WI) and expressed in XL-1 Blue cells (Stratagene). For GST pull down assays, approximately 3 μg of GST-421 and GST protein alone were coupled to glutathione agarose beads (Sigma-Aldrich) and incubated with 0.5 ml cell extract expressing biotinylated Skeletor (Bio-Skel) in immunoprecipitation (ip) buffer (20 mM Tris-HCl pH 8.0, 10 mM EDTA, 1 mM EGTA, 150 mM NaCl, 0.1% Triton X-100, 0.1% Nonidet P-40, 1 mM Phenylmethylsulfonyl fluoride, and 1.5 μg Aprotinin) overnight at 4°C. The protein complex coupled beads were washed with 1 ml of IP buffer and analyzed by SDS–PAGE and Western blotting using Streptavidin tagged Alkaline Phosphatase according to the manufacturer's instructions (Promega). Similarly for avidin pull down assays, Bio-Skel or the biotinylation tag alone was bound to immobilized Streptavidin beads (Pierce, Rockford, IL) and incubated with 3 μg of GST-421 in 50 μl of immunoprecipitation buffer. The resulting complexes were then analyzed by SDS–PAGE and Western blotting using anti-GST antibody.

Immunoprecipitation assays. For co-immunoprecipitation experiments, anti-Skeletor or anti-Chromator antibodies were coupled to protein A beads (Sigma-Aldrich) as follows: 10 μl of Bashful anti-Skeletor serum or 10 μl of mAb 6H11 was coupled to 30 μl protein-A Sepharose beads (Sigma-Aldrich) for 2.5 h at 4°C on a rotating wheel in 50 μl ip buffer. The appropriate antibody-coupled beads or beads only were incubated overnight at 4°C with 200 μl of 0–3 h embryonic lysate on a rotating wheel. Beads were washed 3 times for 10 min each with 1 ml of ip buffer with low speed pelleting of beads between washes. The resulting bead-bound immunocomplexes were analyzed by SDS–PAGE and Western blotting according to standard techniques [Harlow and Lane, 1988] using mAb 6H11 to detect Chromator.

Immunohistochemistry

Antibody labelings of 0–3 h embryos were performed as previously described [Johansen et al., 1996; Johansen and Johansen, 2003]. The embryos were dechorionated in a 50% Chlorox solution, washed with 0.7 M NaCl/0.2% Triton X-100 and fixed in a 1:1 heptane:fixative mixture for 20 min with vigorous shaking at room temperature. The fixative was either 4% paraformaldehyde in phosphate buffered saline (PBS) or Bouin's fluid (0.66% picric acid, 9.5% formalin, 4.7% acetic acid). Vitelline membranes were then removed by shaking embryos in heptane-methanol [Mitchison and Sedat, 1983] at room temperature for 30 s. S2 cells were affixed onto poly-L-lysine coated coverslips and fixed with Bouin's fluid for 10 min at 24°C and methanol for 5 min at −20°C. The cells on

the coverslips were permeabilized with PBS containing 0.5% Triton X-100 and incubated with diluted primary antibody in PBS containing 0.1% Triton X-100, 0.1% sodium azide, and 1% normal goat serum for 1.5 h. Double and triple labelings employing epifluorescence were performed using various combinations of antibodies against Chromator (mAb 6H11, IgG1), Skeletor (mAb 1A1, IgM), anti-α-tubulin mouse IgG1 antibody (Sigma-Aldrich), V5-antibody (IgG2A), GFP-antibody (rabbit polyclonal serum), and Hoechst to visualize the DNA. The appropriate TRITC-, and FITC-conjugated secondary antibodies (Cappel/ICN) were used (1:200 dilution) to visualize primary antibody labeling. Confocal microscopy was performed with a Leica confocal TCS NT microscope system equipped with separate Argon-UV, Argon, and Krypton lasers and the appropriate filter sets for Hoechst, FITC, and TRITC imaging. A separate series of confocal images for each fluorophor of double labeled preparations were obtained simultaneously with z-intervals of typically 0.5 μm using a PL APO 100X/1.40–0.70 oil objective. A maximum projection image for each of the image stacks was obtained using the ImageJ software. In some cases individual slices or projection images from only two to three slices were obtained. Images were imported into Photoshop where they were pseudocolored, image processed, and merged. In some images non-linear adjustments were made for optimal visualization especially of Hoechst labelings of nuclei and chromosomes. Polytene chromosome squash preparations from late third instar larvae were immunostained by the Skeletor antibody mAb 1A1 and Chromator antibody mAb 6H11 essentially as previously described by Zink and Paro [1989] and by Jin et al. [1999].

Expression of Chromator Constructs in Transfected S2 Cells

A full length Chromator (926 aa) construct was cloned into the pMT/V5-HisB vector (Invitrogen) with and without a GFP tag in-frame at the NH_2-terminus and an in-frame V5 tag at the COOH-terminal end using standard methods [Sambrook et al., 1989]. The NH_2-terminal domain of Chromator from residue 1 to 346, containing the chromodomain, was subcloned into the pMT/V5-HisA vector (Invitrogen) with an in-frame V5-tag at the COOH-terminal. Similarly a COOH-terminal domain of Chromator from residue 329 to 926 was subcloned into the pMT/V5-HisB vector (Invitrogen) with an in-frame GFP tag at the NH_2-terminus or with a V5-tag at the COOH-terminus using standard methods [Sambrook et al., 1989]. The fidelity of all constructs was verified by sequencing at the Iowa State University Sequencing facility.

Drosophila Schneider 2 (S2) cells were cultured in Shields and Sang M3 insect medium (Sigma-Aldrich) supplemented with 10% fetal bovine serum, antibiotics and L-Glutamine at 25°C. The S2 cells were transfected with different Chromator subclones using a calcium phosphate transfection kit (Invitrogen) and expression was induced by 0.5 mM $CuSO_4$. Cells expressing Chromator constructs were harvested 18–24 h after induction and affixed onto poly-L-lysine coated coverslips for immunostaining and Hoechst labeling.

RNAi Interference

dsRNAi in S2 cells was performed according to Clemens et al. [2000]. A 780 bp fragment encoding the 5′ end of Chromator cDNA was PCR amplified and used as templates for in vitro transcription using the Megascript™ RNAi kit (Ambion, Austin, TX). Forty microgram of synthesized dsRNA was added to 1×10^6 cells in 6-well cell culture plates. Control dsRNAi experiments were performed identically except pBluescript vector sequence (800 bp) was used as template. The dsRNA treated S2 cells were incubated for 120 h and then processed for immunostaining and immunoblotting. For immunoblotting 10^5 cells were harvested, resuspended in 50 μl of S2 cell lysis buffer (50 mM Tris-HCl pH 7.8, 150 mM NaCl, and 1% Nonidet P-40), boiled and analyzed by SDS–PAGE and Western blotting with anti-Chromator antibody (mAb 6H11), anti-α tubulin antibody.

Analysis of P-Element Mutants

Viability assays. The effect on viability of each P insert was tested by examining the survival rate of the progeny of a $y^1\ w^{1118}$; *KG06256*/*TM6*, Sb^1, Tb^1, *e* stock and a $y^1\ w^{1118}$; *KG03258*/*TM6*, Sb^1, Tb^1, *e* stock. For these assays eggs were collected on standard yeasted agar plates and incubated at 21°C. Hatching viability was measured by counting the number of unhatched eggs after 48 h. Given that 1/4 of the eggs do not hatch due to TM6/TM6 embryonic lethality, the

results from both stocks indicate that there is no significant embryonic lethality of *KG03258*/*KG03258* (0.735 hatching rate) or *KG06256*/*KG06256* (0.720 hatching rate) individuals produced by heterozygous mothers. To measure survival to the adult stage larvae were collected shortly after hatching and allowed to develop. The number of heterozygote adults (*Sb*) was compared with the number of homozygotes (Sb^+). The ratio of *KG03258*/*KG03258* to heterozygotes (0/479) and *KG06256*/*KG06256* to heterozygotes (0/399) indicates that larvae homozygous for either P insertion do not survive to the adult stage.

Complementation analysis. The two P inserts were tested in a standard reciprocal cross complementation test to determine whether they affect the same lethal function. Males from a $y^1\ w^{1118}$; *KG03258*/*TM3*, Sb^1, Ser^1 stock were crossed with females from a $y^1\ w^{1118}$; *KG06256*/*TM6*, Sb^1, Tb^1, *e* stock or vice versa. The progeny were scored for surviving adults that had a Sb^+ phenotype, which should have been *KG06256*/*KG03258*. The expected Mendelian ratio of Sb^+ to *Sb*, assuming complete complementation would be 1:2. The observed numbers from two combined crosses was 1:2.1 (197:420). This is not statistically different from the expected numbers ($P > 0.1$ Chi-square test).

P-element excision. The SUPor-P element of y^1; *P* {$y^{+mDint2}\ w^{BR.E.BR} = SUPor\text{-}P$}*KG03258 ry506*/*TM3*, Sb^1Ser^1 was mobilized by a Δ2–3 transposase source (*y w; Δ2-3Sb*/*TM2Ubx e*) [Robertson et al., 1988]. Several fly lines in which the SUPor-P element had been excised were identified by their white eye color. Three precise excisions were confirmed by polymerase chain reaction (PCR) analysis using primers corresponding to the SUPor-P element and/or the genomic sequences flanking it. DNA isolation from single flies and PCR reaction were performed as described in Preston and Engels [1996]. The precise excision lines were further analyzed for viability as described above and for restoration of Chromator protein levels by immunoblotting. Protein extracts were prepared by homogenizing crawling second instar larvae in IP buffer. Homozygous *KG03258* larvae were identified by the absence of the *tubby* marker. Proteins were separated on SDS–PAGE and analyzed by Western blotting with anti-Chromator antibody (mAb 6H11) and anti-α tubulin antibody.

RESULTS

The Putative Spindle Matrix Protein Skeletor Interacts With a Novel Chromodomain Protein

In order to identify candidates for proteins comprising the putative spindle matrix macromolecular complex we conducted yeast two-hybrid interaction assays using a Skeletor bait construct containing amino acids 215 through 474 that alone was unable to activate transcription of the reporter genes. Two different embryonic yeast two-hybrid libraries were screened (0–2 and 0–21 h) and two interacting clones comprised of partial *CG10712* coding sequences were identified, one from each library. We then sequenced several ESTs corresponding to this locus and assembled the complete 926 amino acid sequence of the gene (Fig. 1A). Analysis of the isolated Chromator yeast two-hybrid library clones suggest that the interaction region with Skeletor is COOH-terminally located between residue 601 and 926 (Fig. 1B). In addition, we identified at least three alternative transcripts due to variant use of different 5′ exons as depicted in Figure 1B. Each transcript, however, contains the same putative start codon and open reading frame (ORF) suggesting the alternative transcripts encode identical gene products. Although 5′ to the ATG-containing exon there is alternative exon usage, 3′ to the ATG-containing exon the exons are invariant. Residues 216–260 of the predicted protein encode a chromodomain [Paro and Hogness, 1991; reviewed in Eissenberg, 2001] (black box in Fig. 1B) and for this reason we named the protein Chromator. Outside of the chromodomain, Chromator does not contain any previously described conserved motifs.

We generated four different mAbs against Chromator, mAb 6H11, mAb 8D12, mAb 6A2, and mAb 12H9. All four antibodies recognize a doublet band migrating at approximately 130 kD (as exemplified by mAb 6H11 in Fig. 1C) which is slightly larger but consistent with the predicted molecular mass of Chromator of 101 kD. The 130 kD doublet band immunoreactivity is specifically competed away if the antibodies are preadsorbed with a GST-Chromator fusion protein but not with GST alone (data not shown) supporting the specificity of the antibodies. The doublet indicates that Chromator may undergo posttranslational modifications and it is possible that such modifications regulate the interaction between

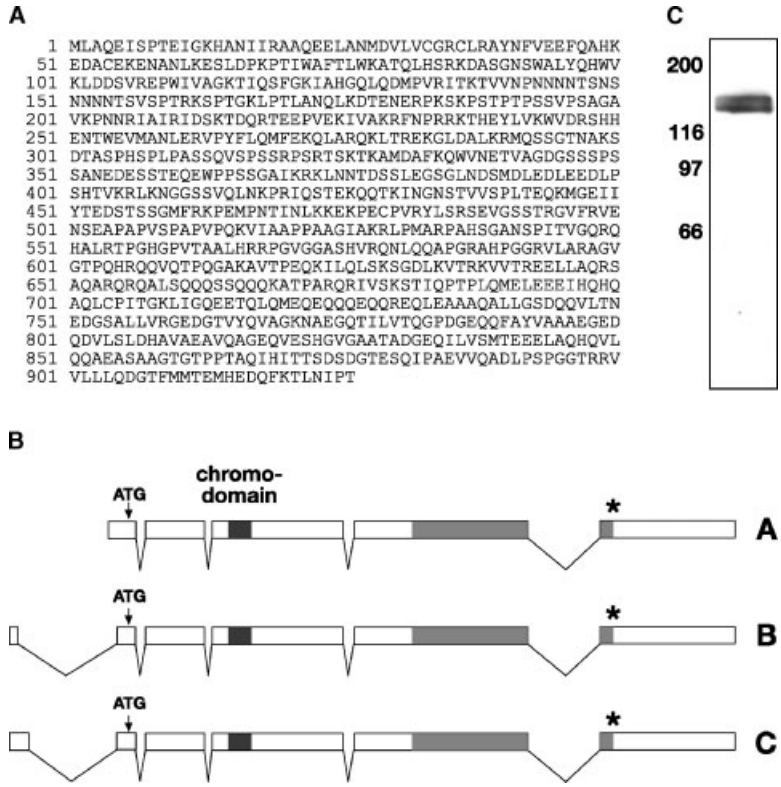

Fig. 1. The organization and protein coding potential of the *Chromator* locus. **A**: The complete predicted amino acid sequence of Chromator. Chromator is a 926 residue protein with a calculated molecular mass of 101 kD. Residues 216–260 encodes a chromodomain. **B**: Diagram of *Chromator* alternative transcripts. The *Chromator* locus gives rise to at least three different transcripts (A, B, and C). Each transcript, however, contains the same putative start codon and open reading frame (ORF) suggesting the alternative transcripts encode identical gene products. The location of the chromodomain is indicated by a black box, the region that includes the Skeletor interaction domain by a grey box, and the location of the stop codon by an asterisk. **C**: Western blot analysis of *Drosophila* embryonic protein extract shows that mAb 6H11 recognizes Chromator protein as a doublet of approximately 130 kD. The migration of molecular weight markers are indicated to the left.

Chromator and Skeletor. To confirm the physical interaction with Skeletor, we performed in vitro pull down experiments using a PinPoint vector (Promega) construct that produces biotinylated Skeletor fusion protein and GST-Chromator fusion protein produced in *E. coli*. Whereas the biotinylation target peptide encoded by the PinPoint vector alone was not able to pull down Chromator when purified using avidin beads, biotinylated Skeletor PinPoint fusion protein pulled down a band corresponding to the size of GST-Chromator (Fig. 2A). In the converse experiment, GST-Chromator fusion protein was able to pull down biotinylated Skeletor using GST-beads whereas GST protein alone was not (Fig. 2B). These results support the existence of a direct physical interaction between Skeletor and Chromator. In addition, we performed co-immunoprecipitation experiments using embryonic lysates in order to address whether Chromator and Skeletor can interact in vivo. For these experiments proteins were extracted from *Drosophila* embryos, immunoprecipitated with Skeletor or Chromator antibody, fractionated on SDS–PAGE after the immunoprecipitation, immunoblotted, and probed with antibody to Chromator. Figure 2C shows such an immunoprecipitation experiment where the immunoprecipitate of both Chomator and Skeletor antibody was detected as an identical 130 kD band that was also present in the embryo lysate. This band was not present in lanes where immunobeads only were used for the immunoprecipitation. These results provide further evidence that Chromator and Skeletor are present in the same protein complex.

Localization of Chromator During the Cell Cycle

Skeletor localizes to chromatin during interphase and to a spindle-like structure during late

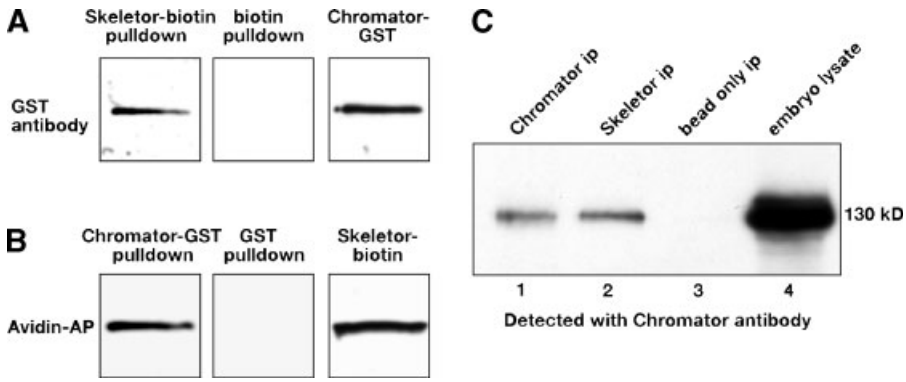

Fig. 2. Chromator and Skeletor pull-down and immunoprecipitation assays. **A**: A Skeletor-biotin construct pulls down Chromator-GST as detected by GST antibody (**lane 1**). A biotin only pulldown control was negative (**lane 2**). **Lane 3** shows the position of the Chromator-GST fusion protein. **B**: A Chromator-GST construct pulls down biotinylated Skeletor as detected by Streptavidin alkaline phosphatase (Avidin-AP) (**lane 1**). A GST only pull down control was negative (**lane 2**). **Lane 3** shows the position of the Skeletor-biotin fusion protein. **C**: Immunoprecipitation (ip) of lysates from *Drosophila* embryos were performed using Chromator antibody (mAb 6H11, **lane 1**) and Skeletor antibody (Bashful antiserum, **lane 2**) coupled to immunobeads or with immunobeads only as a control (**lane 3**). The immunoprecipitations were analyzed by SDS–PAGE and Western blotting using Chromator mAb 6H11 for detection. Chromator antibody staining of embryo lysate is shown in **lane 4**. Chromator is detected in the Skeletor and Chromator immunoprecipitation samples as a 130 kD band (lane 2 and 1, respectively) but not in the control sample (lane 3).

prophase through anaphase [Walker et al., 2000]. Thus, it is possible that selection for interaction partners of Skeletor would identify other chromatin-specific proteins in addition to those involved in spindle or spindle matrix functions. For this reason it was important to examine Chromator's distribution during the cell cycle. Therefore we performed double labelings using mAb 6H11 (IgG1) anti-Chromator and mAb 1A1 (IgM) anti-Skeletor antibodies on fixed syncytial blastoderm embryos at different stages of mitosis. Figure 3 shows that Chromator co-localizes with Skeletor during interphase and reorganizes to form a spindle at metaphase that co-localizes with the Skeletor spindle. However, it should be noted that at this stage Chromator is also found on the centrosomes. A further distinction between the Skeletor and Chromator localization patterns is evident at telophase when Skeletor begins to redistribute to the decondensing chromosomes whereas at this stage the majority of Chromator is localized to the spindle midbody with significant levels also observed at the centrosomes.

We also more closely analyzed Chromator's interphase distribution by triple labeling chromosome squash preparations of late third instar larval polytene chromosomes with anti-Chromator and anti-Skeletor antibodies and with Hoechst to visualize the DNA. Figure 4 shows an example of such an experiment in which Chromator was found to localize to many distinct bands on the chromosomes (Fig. 4A). Anti-Skeletor antibody labeling also shows a large number of chromosomal bands as well as nucleolar staining (Fig. 4B). Although the nucleolus and some of the Skeletor-positive bands do not co-localize with Chromator, all of the Chromator-labeled bands are also found to label with anti-Skeletor antibody, as shown in the composite labeling panel (Fig. 4E). Interestingly, the localization of the Chromator and Skeletor antibody labeled chromatin bands correspond to interband regions with only very limited overlap to regions of strong Hoechst staining (Fig. 4C) suggesting that the two proteins are associated with regions of euchromatin where the majority of active genes reside (Fig. 4D,F).

The spindle localization of Chromator is not restricted to the early embryonic cycles of nuclear division that lack the normal cell cycle checkpoints. We analyzed Chromator distribution in the S2 cell line which is a cell line that was originally derived from later stage embryonic cells (~16 h). In these cells, Chromator shows a similar distribution pattern to that of syncytial blastoderm embryos (Fig. 5). At interphase Chromator co-localizes with Skeletor in the nuclei (Fig. 5, upper panel) whereas at metaphase Chromator and Skeletor are co-localized at a spindle-like structure distinct from the chromosomes congregated at the metaphase plate (Fig. 5, middle panel). However, in

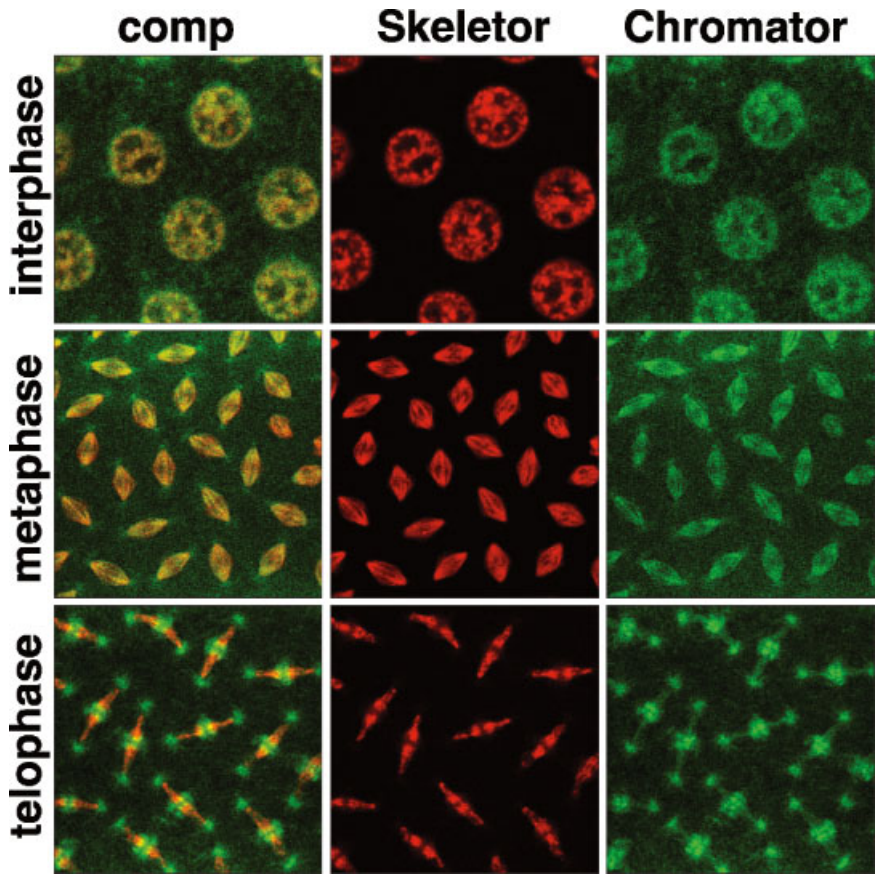

Fig. 3. The dynamic redistribution of Chromator relative to Skeletor during the cell cycle in *Drosophila* embryos. The composite images (comp) show extensive overlap between Chromator (green) and Skeletor (red) labeling at inter-, meta-, and telophase as indicated by the predominantly yellow color. However, the distribution is not identical. In contrast to Skeletor, Chromator is present on centrosomes and appears to be preferentially localized to the spindle midbody at telophase. All images in these panels are from confocal sections of syncytial embryonic nuclei double labeled with mAb 6H11 (Chromator) and mAb 1A1 (Skeletor). [Color figure can be viewed in the online issue, which is available at www.interscience.wiley.com.]

contrast to Skeletor-labeling which does not extend to the centrosomes Chromator-labeling extends all the way to the spindle poles and includes centrosomes. At late telophase both Chromator- and Skeletor-labeling associates with the reforming daughter nuclei while an appreciable level of Chromator-labeling was also found at the midbody region (Fig. 5, lower panel).

Chromator is an Essential Gene

Two SUPor-P [Roseman et al., 1995] elements have been found to be inserted into the *CG10712* region between the predicted Chromator coding sequence and a second gene *ssl1* transcribed from the opposite strand (Fig. 6A). We verified the P-element insertion sites by PCR analysis using primers corresponding to genomic sequences flanking the region and sequencing the PCR product. In *KG03258* flies the P-element is inserted within the first intron of Transcript B and Transcript C and 50 bp before the first exon of Transcript A (Fig. 6A). In *KG06256* flies the P-element is inserted 5′ to the initiation sites of the first exon for both Transcripts B and C. We analyzed the effect on viability (see "Materials and Methods") of both insertions and found that each is homozygous lethal with *KG03258* animals not surviving past 2nd instar larval stages and *KG06256* animals dying during larval and pupal stages. However, complementation analysis shows that *KG03258*/*KG06256* animals are viable (see "Materials and Methods") indicating that these alleles can complement and that they, therefore, either affect different genes or they affect a gene exhibiting complex complementation. That they affect different genes would be consistent with the

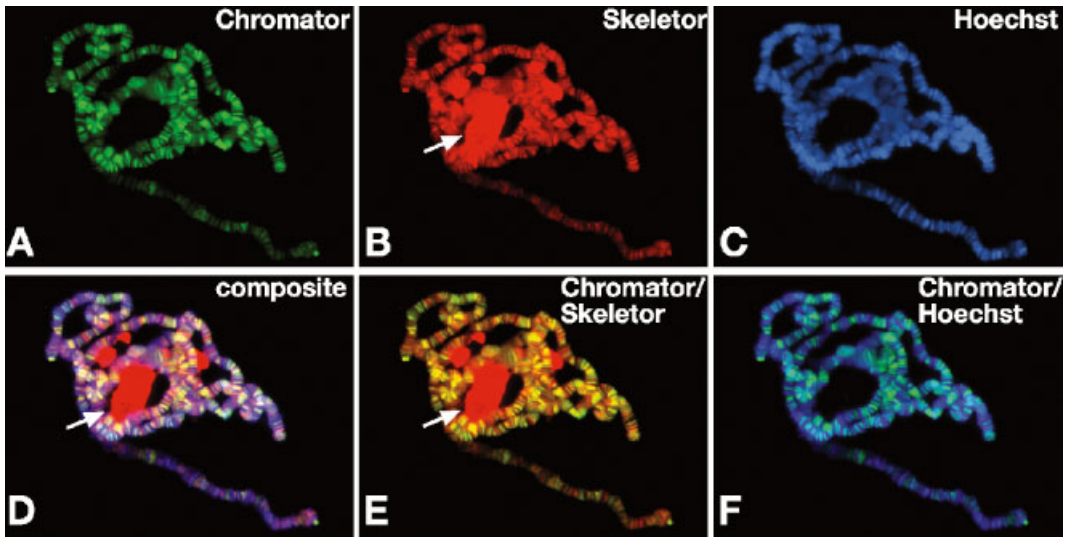

Fig. 4. Chromator expression in salivary gland polytene chromosomes. **A–F**: Triple labelings using mAb 6H11 to visualize Chromator (green), mAb 1A1 to visualize Skeletor (red), and Hoechst to visualize the DNA (blue) reveal that Chromator and Skeletor co-localize to a large number of chromosome bands (yellow in E). While Skeletor antibody additionally labels the nucleolus (arrow in B, D, and E) and is present on a subset of bands not labeled by Chromator antibody, all Chromator-positive bands are also Skeletor-antibody positive (E). In the composite image (F) there is little overlap between Chromator (green) and Hoechst (blue) labeling. (A) Chromator-labeling, (B) Skeletor-labling, (C) Hoechst-labeling, (D) composite of Chromator-, Skeletor-, and Hoechst-labeling, (E) composite of Chromator- and Skeletor-labeling, (F) composite of Chromator- and Hoechst-labeling. [Color figure can be viewed in the online issue, which is available at www.interscience.wiley.com.]

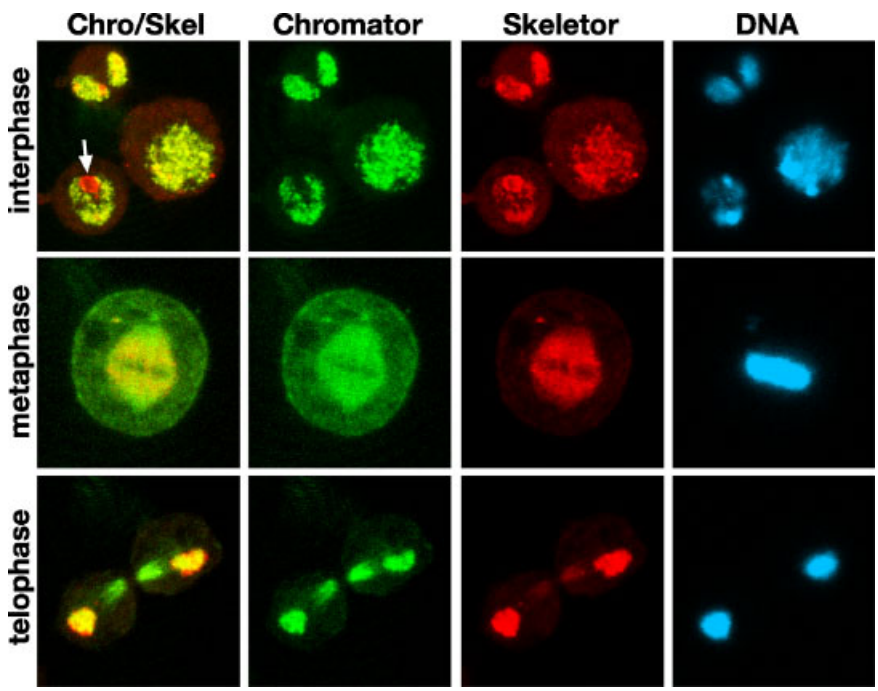

Fig. 5. The dynamic redistribution of Chromator relative to Skeletor during the cell cycle in *Drosophila* S2 cells. The composite images (Chro/Skel) show extensive overlap between Chromator (green) and Skeletor (red) labeling at inter-, meta-, and telophase as indicated by the predominantly yellow color. However, the distribution is not identical. In contrast to Skeletor, Chromator is present on centrosomes and appears to be preferentially localized to the spindle midbody at telophase. In addition at interphase the nucleolus is labeled by Skeletor-antibody (arrow). All images in these panels are from confocal sections of S2 cells triple labeled with mAb 6H11 (Chromator), mAb 1A1 (Skeletor), and Hoechst (DNA). [Color figure can be viewed in the online issue, which is available at www.interscience.wiley.com.]

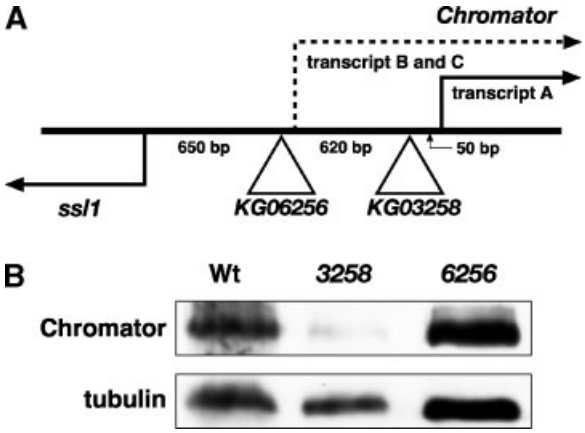

Fig. 6. P-element insertions in the *Chromator* locus. **A**: The insertion sites of two P-elements, *KG06256* and *KG03258*, in the region of Chromator transcript initiation. A second gene, *ssl1*, could potentially be affected by one or both of these insertions. **B**: Western blot with Chromator antibody of extracts from homozygous *KG06256* and *KG03258* larvae as compared to wild type. Tubulin antibody labeling is shown below as a loading control. The Chromator protein level was severely reduced as compared to wild type levels in *KG03258* (*3258*) larvae whereas *KG06256* (*6256*) larvae had levels comparable to that of wild type larvae.

genomic organization in the region with the *ssl1* gene being transcribed from the opposite strand just upstream from the *Chromator* gene (Fig. 6A).

In order to determine which P-element insertion affects the *Chromator* gene, we fractionated proteins from wild-type or homozygous mutant second or third instar larval extracts on SDS–PAGE gels, Western blotted the proteins onto nitrocellulose, and probed with mAb 6H11 anti-Chromator antibody (Fig. 6B). Homozygous *KG06256* third instar larvae contained near wild-type levels of Chromator protein ($93.3 \pm 11.0\%$, $n = 6$), whereas the few *KG03258* animals surviving to 2nd instar stages lacked or had severely reduced Chromator protein levels ($2.2 \pm 2.1\%$, $n = 6$) (Fig. 6B). Any residual protein observed likely reflects remaining maternally-derived Chromator since significant levels of Chromator protein were present in 0–2 h embryos (data not shown). Thus, the stage of 2nd instar lethality for homozygous *KG03258* mutant animals correlates well with the loss of Chromator protein in these animals. Based on these results, we propose that *KG03258* is a lethal loss-of-function mutation in the *Chromator* gene. The presence of abundant Chromator protein in the homozygous *KG06256* mutant suggests the lethality of this mutation is likely due to the neighboring *ssl1* gene. Furthermore, based on the complementation analysis *ssl1* gene function does not appear to be affected by the *KG03258* P-element insertion.

In a recent study, it was found that in a significant percentage of lethal mutant lines carrying characterized P insertions, the lethal mutation was not directly associated with the P insertion event itself [Bellotto et al., 2002]. For this reason it was essential to confirm that the P insertion is the source of lethality for the *KG03258* allele. In order to address this concern, we screened for precise excision events by introducing the $\Delta 2-3$ transposase to mobilize the transposon and then selecting for loss of the mini-white and yellow markers that are carried by the SUPor-P element. Stocks established from such flies were then analyzed by PCR to characterize the nature of the excision event to identify those lines with precise excisions of the P-element. Test crosses of such lines demonstrated that the precise excision of the SUPor-P element restored Chromator expression and viability to flies that were homozygous for the third chromosome that had previously carried the *KG03258* insertion (data not shown). That precise excision of the *KG03258* SUPor-P element restores Chromator expression and viability supports that the lethality observed in the *KG03258* mutant line was directly due to the insertion of the P-element in the *Chromator* region.

Functional Consequences of Reduced Chromator Protein Levels

The yeast two-hybrid, pull-down, and immunolabeling results are consistent with that Skeletor and Chromator physically interact, although we cannot at present distinguish whether this interaction occurs at interphase, during mitosis, or both. However, the Chromator distribution pattern and its co-localization with Skeletor during metaphase suggest that Chromator has the potential to play a functional role in chromosome segregation during mitosis. Unfortunately, this hypothesis cannot be tested in homozygous *KG03258* embryos due to the presence of maternally derived Chromator protein which masks any potential phenotypes. Furthermore, these animals die as early second instar larvae before brain squashes of dividing neuroblasts can be reliably analyzed. For these reasons, we employed RNAi methods in S2 cells to deplete Chromator protein levels and to assay

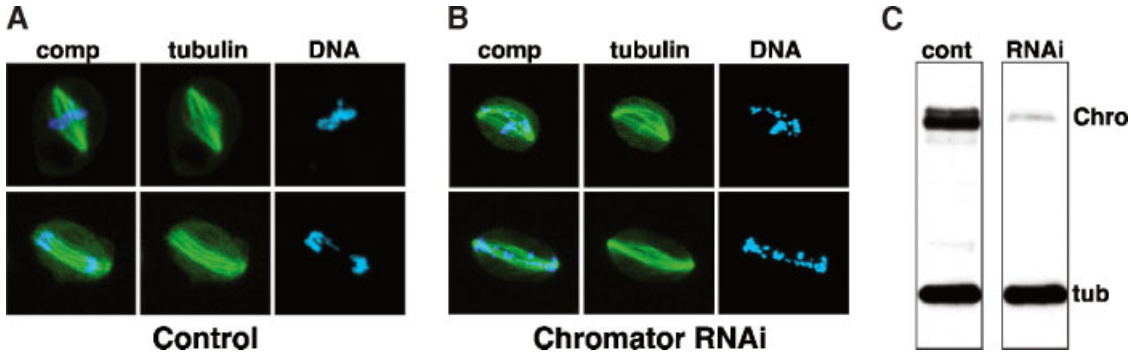

Fig. 7. RNAi depletion of Chromator in S2 cells leads to microtubule spindle abnormalities and chromosome segregation defects. **A**: Examples of control-treated S2 cells at meta- and anaphase. **B**: Examples of Chromator dsRNA treated S2 cells. The upper panel shows an S2 cell in metaphase with a curved microtubule spindle and mis-positioned chromosomes. The lower panel shows the most common phenotype of abnormally narrow spindles and missegregated or misalingned chromosomes scattered throughout the spindle-region. Tubulin antibody-labeling is shown in green and Hoechst labeling of the DNA is in blue. All images in (A) and (B) are from confocal sections of S2 cells. **C**: Western blot with Chromator antibody of control treated and Chromator RNAi treated S2 cells from the cultures shown in (A) and (B). In the RNAi sample Chromator protein levels (Chro) is reduced to about 15% of the level observed in the control cells. Tubulin levels (tub) are shown as a loading control. [Color figure can be viewed in the online issue, which is available at www.interscience.wiley.com.]

for phenotypic consequences during cell division of loss of Chromator by anti-tubulin and Hoechst labeling of the cells (Fig. 7). The degree of Chromator knock down in the cultures was determined by immunoblot analysis. In five separate experiments we reduced the Chromator protein level to an average of $27 \pm 15\%$ (range 10–42%) that of mock treated controls. In these experimental cell cultures we observed numerous examples of spindle and chromosome segregation defects, including misshapen spindles and misaligned and/or lagging chromosomes (Fig. 7B) that were rarely observed in control cells mock treated with pBluescript vector sequence dsRNA. We quantified the difference between experimental and control treated cells by counting the number of such phenotypes in fields of constant size in each of the cultures. Experimental fields had 178 ± 43, $n = 5$ phenotypes versus 5 ± 1, $n = 5$ in control fields. This difference is statistically significant on the $P < 0.001$ level (Student's t-test). However, we did not observe any obvious perturbations of nuclear or chromatin structure in interphase S2 cell nuclei. These results suggest that depletion of Chromator results in severe chromosome segregation defects as well as spindle abnormalities in S2 cells and supports the hypothesis that Chromator plays a functional role in mitosis. Similar experiments were carried out with Skeletor dsRNA; however, no phenotypes were observed (data not shown).

The COOH-Terminal Fragment of Chromator is Sufficient for Nuclear and Spindle Localization

Sequence analysis of Chromator identified only one previously known motif or domain, the chromodomain. Chromodomains (chromatin organization modifier domains) were first described by Paro and Hogness [1991] and are as the name implies generally thought to be involved in mediating associations with chromatin [Brehm et al., 2004]. We, therefore, tested whether the chromodomain plays a role in the localization of Chromator to the nucleus. We made three kinds of constructs containing Chromator sequences for expression in S2 cells carrying either an NH_2-terminal GFP-tag, a COOH-terminal V5-tag, or both. The three constructs were a full length Chromator construct (FL-Chr), an NH_2-terminal construct (NT-Chr) containing sequence from the starting methionine to residue 346 that includes the chromodomain, and a COOH-terminal construct (CT-Chr) from residue 329 to the terminal tyrosine residue without the chromodomain. Identical results were obtained with GFP- and/or V5-tagged constructs. Figure 8 shows examples of expression of these constructs in transiently or stably transfected S2 cells. The GFP-FL-Chr-V5 construct localizes to the nucleus although its overexpression often leads to aggregation (Fig. 8A). The NT-Chr-V5

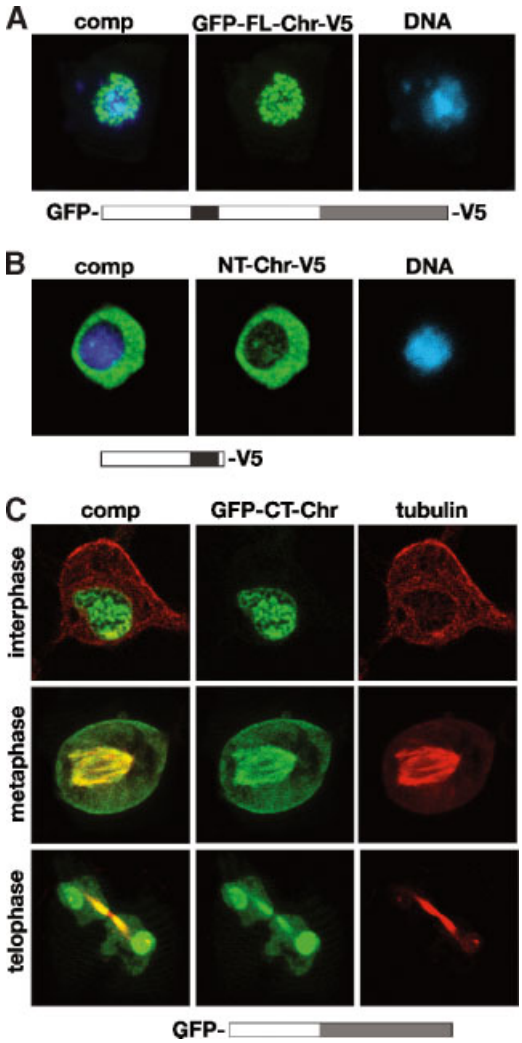

Fig. 8. Expression of Chromator deletion constructs in S2 cells. The expressed constructs are diagrammed beneath the micrographs. **A**: Full-length GFP- and V5-tagged Chromator (GFP-FL-Chr-V5) localizes to the nucleus of S2 cells. The cells were double-labeled with GFP-antibody to visualize the GFP-FL-Chr-V5 construct (green) and Hoechst to visualize the DNA (blue). **B**: V5-tagged NH_2-terminal Chromator deletion construct (NT-Chr-V5) truncated just after the chromodomain (black box) localizes to the cytoplasm and is mainly absent from the nucleus. The NT-Chr-V5 construct was visualized with V5-antibody (green) and the DNA with Hoechst (blue). **C**: S2 cells expressing a GFP-tagged COOH-terminal deletion construct (GFP-CT-Chr) without the chromodomain at inter-, meta-, and telophase. The GFP-CT-Chr construct was visualized with GFP-antibody (green) and microtubules with tubulin-antibody (red). At interphase GFP-CT-Chr localizes to the nucleus whereas at metaphase it co-localizes with the microtubule spindle. At telophase it is localized at the reforming daughter nuclei in addition to co-localizing with microtubules at the midbody. The region that contains the Skeletor interaction domain is indicated in grey. [Color figure can be viewed in the online issue, which is available at www.interscience.wiley.com.]

construct containing the chromodomain is not targeted to the nucleus and remains in the cytoplasm (Fig. 8B). GFP alone localizes to the cytoplasm (data not shown). In contrast, the GFP-CT-Chr construct is localized to the nucleus at interphase, co-localizes with the tubulin spindle at metaphase, and is present at the midbody overlapping with tubulin while redistributing to the forming daughter nuclei at telophase (Fig. 8C). Thus the localization of the COOH-terminal Chromator construct during the cell cycle phenocopies that of endogenous Chromator observed with Chromator antibody labeling. This indicates that the chromodomain is not necessary for targeting of Chromator to the nucleus but rather that COOH-terminal sequences are sufficient for both nuclear and spindle localization.

DISCUSSION

In this study we provide evidence that the putative spindle matrix protein Skeletor molecularly interacts with a novel chromodomain containing protein, Chromator. This interaction was first detected in a yeast two-hybrid screen and subsequently confirmed by pull-down assays. Furthermore, immunocytochemical labeling of *Drosophila* embryos, S2 cells, and polytene chromosomes demonstrate that the two proteins show extensive co-localization during the cell cycle although their distributions are not identical. During interphase Chromator is localized on chromosomes to interband chromatin regions in a pattern that overlaps that of Skeletor. However, a major difference is that Skeletor, unlike Chromator, also is present in the nucleolus. During mitosis both Chromator and Skeletor detach from the chromosomes and align together in a spindle-like structure with Chromator additionally being localized to centrosomes that are devoid of Skeletor-antibody labeling. During telophase both proteins redistribute to the forming daughter nuclei with appreciable levels of Chromator immunoreactivity also present at the midbody region. The extensive co-localization of the two proteins is compatible with a direct physical interaction between Skeletor and Chromator. However, at present we do not know whether such an interaction occurs throughout the cell cycle or is present only at certain stages with additional proteins mediating complex assembly at other stages.

The co-localization of Chromator with the Skeletor-defined spindle matrix during mitosis suggests that Chromator may be involved in spindle matrix function. A spindle matrix has been hypothesized to provide a stationary substrate that anchors motor molecules during force production and microtubule sliding [Pickett-Heaps et al., 1997]. Although theoretical calculations have been derived in support of a hypothesis that observed spindle dynamics can be satisfactorily accounted for based on a structure comprised solely of microtubules and motors [Sharp et al., 2000; Scholey et al., 2001; Cytrynbaum et al., 2003], direct evidence that motor proteins can be static in bipolar spindles relative to tubulin has been provided by flux experiments with the mitotic kinesin Eg5 in *Xenopus* [Kapoor and Mitchison, 2001]. These flux experiments were interpreted as revealing the existence of a static, non-microtubule mechanical scaffold that transiently anchors Eg5 within spindles [Kapoor and Mitchison, 2001]. Thus, a prediction of the spindle matrix hypothesis is that if such a scaffold was interfered with in a way that it could not properly anchor motor proteins, it would affect the dynamic behavior of spindle components such as motors and lead to abnormal chromosome segregation.

The identification and characterization of the Skeletor protein in *Drosophila* was the first molecular evidence for the existence of a complete spindle matrix that forms within the nucleus [Walker et al., 2000]. However, as no Skeletor mutants have been isolated there has been a lack of direct insight into Skeletor's potential role in spindle matrix function. In the present study we show using RNAi assays in S2 cells that depletion of Chromator protein leads to abnormal spindle morphology and that chromosomes are scattered in the spindle indicating defective spindle function in the absence of Chromator. These types of defects would be expected if Chromator functions as a spindle matrix associated protein that promotes interactions between motor proteins and a stationary scaffold and if these interactions were necessary for chromosome mobility. Interestingly, this phenotype resembles the mitotic chromosome segregation defects observed after RNAi knockdown of some kinesin motor proteins in S2 cells including KLP67A by Goshima and Vale [2003] and KLP59C by Rogers et al. [2004]. Thus, these data provide evidence that Chromator is a nuclear derived protein that plays a role in proper spindle dynamics leading to chromosome separation during mitosis and are compatible with the hypothesis that Chromator may constitute a functional component of a spindle matrix molecular complex.

Recently it has become clear that numerous nuclear and chromosome associated proteins play an important role in spindle assembly and function. In vertebrates, other proposed components of a spindle matrix, NuMA and TPX2, are located to the spindle poles at metaphase assisting in stabilizing and focusing microtubules in the region near the centrosomes [Merdes et al., 1996; Dionne et al., 1999; Wittmann et al., 2001]. NuSAP, a nucleolar derived protein was shown to be involved in mitotic spindle organization and to be able to bundle microtubules [Raemaekers et al., 2003]. In cells lacking a centrosome, chromosomes have been found to play a key role in forming spindles [Theurkauf and Hawley, 1992; reviewed in McKim and Hawley, 1995; Karsenti and Vernos, 2001]. A Ran-GTP gradient generated near chromosomes by the chromosomal-associated Ran-GEF RCC1 is responsible for importins α and β to release factors critical for localized microtubule assembly followed by subsequent organization by various motor proteins into a bipolar spindle [Carazo-Salas et al., 2001; Hetzer et al., 2002; reviewed in Wittmann et al., 2001]. Further chromosomal contributions to mitotic regulation have been elaborated in studies of the so-called "chromosomal passenger protein complex" [reviewed in Adams et al., 2001; Terada, 2001]. These proteins have been implicated in chromosome condensation and segregation as well as in completion of cytokinesis.

Chromator is a chromodomain containing protein and is localized to chromatin during interphase. The function of most of the chromodomain proteins identified so far have been related to chromosome structure [Brehm et al., 2004]. For example, HP1 binds to methylated histone H3 and is essential for the assembly of heterochromatin [Nielsen et al., 2001; Peters et al., 2001; Jacobs and Khorasanizadeh, 2002]. The chromodomain of Chromator most closely resembles that of Ppd1 a protein involved in programmed DNA elimination in *Tetrahymena* [Taverna et al., 2002]. It was suggested that Ppd1 functions through association with histone H3 by a mechanism similar to that used by HP1 in maintaining heterochromatin

structure. Thus, a reasonable expectation would be that Chromator also serves a role in establishing or maintaining chromatin structure during interphase. However, in Chromator RNAi assays we did not detect any obvious aberrant phenotypes of nuclear or chromatin structure in S2 cells. Furthermore, deletion construct analysis showed that the chromodomain containing NH_2-terminal part of Chromator was not necessary for nuclear targeting or for localization to the mitotic spindle apparatus. It is, therefore, possible that the COOH-terminal interaction site of Chromator with Skeletor is responsible for its localization during the cell cycle. Interestingly, Skeletor antibody injection into syncytial *Drosophila* embryos leads to nuclear disintegration and fragmented chromatin [Walker et al., 2000]. This suggests that a potential Chromator/Skeletor complex would be likely to play some functional role in maintaining nuclear integrity during interphase and that some aspects of this function may be mediated by Chromator's chromodomain. A caveat is that it has recently become clear that chromodomains may have evolved from a common ancestral fold to fulfill various functions in different molecular contexts that are not necessarily associated with chromatin [Brehm et al., 2004]. Regardless, it is likely that Chromator together with Skeletor functions in at least two different molecular complexes, one associated with a spindle-like structure during mitosis and one associated with nuclear and chromatin structure during interphase. The future isolation and characterization of point and hypomorphic mutations in Chromator promises to resolve these questions and to provide further insights into the function of this protein and the putative spindle matrix.

ACKNOWLEDGMENTS

We thank members of the laboratory for discussion, advice, and critical reading of the manuscript. We also acknowledge Ms. V. Lephart for maintenance of fly stocks and Dr. D. Walker for assistance with generating the mAb 8C7. We thank Dr. H.J. Bellen and Dr. L. Ambrosio and the Bloomington Stock Center for generously providing fly stocks.

REFERENCES

Adams RR, Carmena M, Earnshaw WC. 2001. Chromosomal passengers and the (aurora) ABCs of mitosis. Trends Cell Biol 11:49–54.

Bellen HJ, Levis RW, Liao G, He Y, Carlson JW, Tsang G, Evans-Holm M, Hiesinger PR, Schulze KL, Rubin GM, Hoskins RA, Spradling AC. 2004. The BDGP gene disruption project: Single transposon insertions associated with 40% of *Drosophila* genes. Genetics 167:761–781.

Bellotto M, Bopp D, Senti K-A, Burke R, Deak P, Maroy P, Dickson B, Basler K, Hafen E. 2002. Maternal-effect loci involved in *Drosophila* oogenesis and embryogenesis: P element-induced mutations on the third chromosome. Int J Dev Biol 46:149–157.

Bloom K. 2002. Yeast weighs in on the elusive spindle matrix: New filaments in the nucleus. Proc Natl Acad Sci USA 99:4757–4759.

Brehm A, Tufteland KR, Aasland R, Becker PB. 2004. The many colours of chromodomains. BioEssays 26:133–140.

Carazo-Salas RE, Gruss OJ, Mattaj IW, Karsenti E. 2001. Ran-GTP coordinates regulation of microtubule nucleation and dynamics during mitotic-spindle assembly. Nat Cell Biol 3:228–234.

Clemens JC, Worby CA, Simonson-Leff N, Muda M, Maehama T, Hemmings BA, Dixon JE. 2000. Use of double-stranded RNA interference in *Drosophila* cell lines to dissect signal transduction pathways. Proc Natl Acad Sci USA 97:6499–6503.

Cytrynbaum EN, Scholey JM, Mogilner A. 2003. A force balance model of early spindle pole separation in *Drosophila* embryos. Biophys J 84:757–769.

Dionne MA, Howard L, Compton DA. 1999. NuMA is a component of an insoluble matrix at mitotic spindle poles. Cell Motil Cytoskel 42:189–203.

Eissenberg JC. 2001. Molecular biology of the chromo domain: An ancient chromatin module comes of age. Gene 275:19–29.

Goshima G, Vale RD. 2003. The roles of microtubule-based motor proteins in mitosis: Comprehensive RNAi analysis in the *Drosophila* S2 cell line. J Cell Biol 162:1003–1016.

Harlow E, Lane E. 1988. Antibodies: A laboratory manual. NY: Cold Spring Harbor Laboratory Press. 726p.

Hetzer M, Gruss OJ, Mattaj IW. 2002. The Ran GTPase as a marker of chromosome position in spindle formation and nuclear envelope assembly. Nat Cell Biol 4:E177–E184.

Jacobs SA, Khorasanizadeh S. 2002. Structure of HP1 chromodomain bound to a Lysine 9-methylated histone H3 tail. Science 295:2080–2083.

Jin Y, Wang Y, Walker DL, Dong H, Conley C, Johansen J, Johansen KM. 1999. JIL-1, a novel chromosomal tandem kinase implicated in transcriptional regulation in *Drosophila*. Mol Cell 4:129–135.

Johansen KM, Johansen J. 2002. Recent glimpses of the elusive spindle matrix. Cell Cycle 1:312–314.

Johansen KM, Johansen J. 2003. Studying nuclear organization in embryos using antibody tools. In: Henderson DS, editor. *Drosophila* cytogenetics protocols. Totowa, New Jersey: Humana Press. pp 215–234.

Johansen KM, Johansen J, Baek K-H, Jin Y. 1996. Remodeling of nuclear architecture during the cell cycle in *Drosophila* embryos. J Cell Biochem 63:268–279.

Kapoor TM, Compton DA. 2002. Searching for the middle ground: Mechanisms of chromosome alignment during mitosis. J Cell Biol 157:551–556.

Kapoor TM, Mitchison TJ. 2001. Eg5 is static in bipolar spindles relative to tubulin: Evidence for a static spindle matrix. J Cell Biol 154:1125–1133.

Karsenti E, Vernos I. 2001. The mitotic spindle: A self-made machine. Science 294:543–547.

Laemmli UK. 1970. Cleavage of structural proteins during assembly of the head of bacteriophage T4. Nature 227: 680–685.

McKim KS, Hawley RS. 1995. Chromosomal control of meiotic cell division. Science 270:1595–1601.

Merdes A, Ramyar K, Vechio JD, Cleveland DW. 1996. A complex of NuMA and cytoplasmic dynein is essential for mitotic spindle assembly. Cell 87:447–458.

Mitchison TJ, Salmon ED. 2001. Mitosis: A history of division. Nat Cell Biol 3:E17–E21.

Mitchison TJ, Sedat J. 1983. Localization of antigenic determinants in whole *Drosophila* embryos. Dev Biol 99: 261–264.

Nielsen AL, Oulad-Abdelghani M, Ortiz JA, Remboutsika E, Chambon P, Losson R. 2001. Heterochromatin formation in mammalian cells: Interaction between histones and HP1 proteins. Mol Cell 7:729–739.

Paro R, Hogness D. 1991. The Polycomb protein shares a homologous domain with a heterochromatin associated protein of *Drosophila*. Proc Natl Acad Sci USA 88:263–267.

Peters AH, O'Carroll D, Scherthan H, Mechtler K, Sauer S, Schöfer C, Weipoltshammer K, Pagani M, Lachner M, Kohlmaier A, Opravil S, Doyle M, Sibilia M, Jenuwein T. 2001. Loss of the Suv39h histone methyltransferase impairs mammalian heterochromatin and genome stability. Cell 107:323–327.

Pickett-Heaps JD, Tippit DH, Porter KR. 1982. Rethinking mitosis. Cell 29:729–744.

Pickett-Heaps JD, Forer A, Spurck T. 1997. Traction fiber: Toward a "tensegral" model of the spindle. Cell Motil Cytoskel 37:1–6.

Preston CR, Engels WR. 1996. P-element induced male recombination and gene conversion in *Drosophila*. Genetics 144:1611–1622.

Raemaekers T, Ribbeck K, Beaudouin J, Annaert W, Van Camp M, Stockmans I, Smets N, Bouillon R, Ellenberg J, Carmeliet G. 2003. NuSAP, a novel microtubule-associated protein involved in mitotic spindle organization. J Cell Biol 162:1017–1029.

Roberts DB. 1986. *Drosophila*: A practical approach. Oxford, UK: IRL Press. 295p.

Robertson HM, Preston CR, Phillis RW, Johnson-Schlitz DM, Benz WK, Engels WR. 1988. A stable genomic source of P element transposase in *Drosophila melanogaster*. Genetics 118:461–470.

Rogers GC, Rogers SL, Schwimmer TA, Ems-McClung SC, Walczak CE, Vale RD, Scholey JM, Sharp DJ. 2004. Two mitotic kinesins cooperate to drive sister chromatid separation during anaphase. Nature 427:364–370.

Roseman RR, Johnson EA, Rodesch CK, Bjerke M, Nagoshi RN, Geyer PK. 1995. A P element containing suppressor of hairy-wing binding regions has novel properties for mutagenesis in *Drosophila melanogaster*. Genetics 141: 1061–1074.

Sambrook J, Fritsch EF, Maniatis T. 1989. Molecular cloning: A laboratory manual. NY: Cold Spring Harbor Laboratory Press. 545p.

Scholey JM, Rogers GC, Sharp DJ. 2001. Mitosis, microtubules, and the matrix. J Cell Biol 154:261–266.

Sharp DJ, Rogers GC, Scholey JM. 2000. Microtubule motors in mitosis. Nature 407:41–47.

Taverna SD, Coyne RS, Allis CD. 2002. Methylation of histone H3 at lysine 9 targets programmed DNA elimination in *Tetrahymena*. Cell 110:701–711.

Terada Y. 2001. Role of chromosomal passenger complex in chromosome segregation and cytokinesis. Cell Struct Funct 26:653–657.

Theurkauf WE, Hawley RS. 1992. Meiotic spindle assembly in *Drosophila* females: Behavior of nonexchange chromosomes and the effects of mutations in the nod kinesin-like protein. J Cell Biol 116:1167–1180.

Towbin H, Staehelin T, Gordon J. 1979. Electrophoretic transfer of proteins from polyacrylamide gels to nitrocellulose sheets: Procedure and some applications. Proc Natl Acad Sci USA 9:4350–4354.

Walker DL, Wang D, Jin Y, Rath U, Wang Y, Johansen J, Johansen KM. 2000. Skeletor, a novel chromosomal protein that redistributes during mitosis provides evidence for the formation of a spindle matrix. J Cell Biol 151:1401–1411.

Wang Y, Zhang W, Jin Y, Johansen J, Johansen KM. 2001. The JIL-1 tandem kinase mediates histone H3 phosphorylation and is required for maintenance of chromatin structure in *Drosophila*. Cell 105:433–443.

Wells WA. 2001. Searching for a spindle matrix. J Cell Biol 154:1102–1104.

Wittmann T, Hyman A, Desai A. 2001. The spindle: A dynamic assembly of microtubules and motors. Nat Cell Biol 3:E28–E34.

Zink B, Paro R. 1989. In vivo binding pattern of a trans-regulator of homoeotic genes in *Drosophila melanogaster*. Nature 337:468–471.